Incorporation of Titanium into the Inorganic Wall of Ordered Porous Zirconium Oxide via Direct Synthesis

Hang-Rong Chen, Jian-Lin Shi,* Wen-Hau Zhang, Mei-Ling Ruan, and Dong-Sheng Yan

State Key Lab of High Performance Ceramics and Superfine Microstructure, Shanghai Institute of Ceramics, Chinese Academy of Sciences, Shanghai 200050, China

Received October 4, 2000. Revised Manuscript Received January 8, 2001

The ordered porous zirconium oxide incorporated with variable amounts of titanium was synthesized via a direct-hydrothermal synthesis procedure. Characterizations by powder X-ray diffraction, nitrogen adsorption, high-resolution transmission electron microscopy, and energy-dispersive, X-ray photoelectron, Raman, and diffuse reflectance ultraviolet spectroscopies have been carried out to study the chemical nature of titanium in the porous ZrO_2 material. The results show that titanium ions are homogeneously dispersed into the framework of ZrO_2, when the amount of titanium doping is less than 20 mol %, which is much higher than that in silica-based materials. At higher titanium loading, nanocrystalline TiO_2 anatase is formed. A suitable amount of titanium is favorable to the thermal stability of the porous zirconium oxide.

1. Introduction

Silica-based, mesoporous materials have attracted intense interest for their high potential applications as chemical separation, catalysts, etc. To generate more effective functions in applications, the pore surface must be modified. Various techniques have been developed to incorporate transition metals into mesoporous silica by hydrothermal procedures or "postsynthesis" grafting methods.[1,2] Of the numerous doping candidates, titanium appears to be most promising for catalytic applications.

Titanium dioxide is well-known as a large-band-gap semiconductor, versatile photocatalyst and shows great catalytic activity in many selective reactions.[3] Incorporation of titania into silica or zeolitic supports has been studied extensively.[4,5] The zeolites, after modification by isomorphous substitution of Si by Ti during the synthesis, are able to perform selective oxidation of organic compounds such as alkanes, alkenes, and alcohols by H_2O_2.[6] Cubic MCM-48 and SBA-15 mesoporous silica molecular sieves incorporated with titanium have recently been reported to have potential as novel catalysts.[7,8] Titanium can also be substituted into the framework of various materials,[9] including some non-silica-based materials such as aluminophosphates.[10]

The discovery[11] of silica-based, mesoporous materials has expanded the possibilities of non-silica-based porous materials, which opens new potential applications in the fields of catalysis and adsorption.[12]

For a variety of reasons, great interests have currently been focused on the study of porous zirconium oxides. As one of the transition-metal oxides, zirconium oxide is known to play an important role as industrial catalyst and catalyst supports for its particular acid catalysis[13] and oxidizing capabilities as well as its good ion-exchange properties.[14] Porous zirconia has been found to possess high surface areas, ordered frameworks, and narrow pore size distributions, giving them potential applications as host structures and more active catalysts for reactions. In addition, some modified zirconia, such as phosphated zirconia, exhibit higher acid strength and activity for acid-catalyzed reactions.[15] Also, the lattice of ZrO_2 can accommodate a variety of dopants. Much of the early work was concentrated on the synthesis of porous zirconia with high surface area. However, in most cases, the thermal stability and the ordering of the porous structure was poor, and few exceptions are ordered porous zirconium oxo phosphate,[16] zirconium oxide sulfate[17], and mesoporous phosphated zirconia.[18] Recently, some works dealing

* Corresponding author. E-mail: jlshi@sunm.shcnc.ac.cn. Fax: 86-21-62513903.

(1) Xu, J.; Luan, Z.; Hartmann, M.; Kevan, L. *Chem. Mater.* **1999**, *11*, 2928.
(2) Corma, A.; Jorda, J. L.; Navarro, M. T.; Rey, F. *Chem. Commun.* **1998**, 1899.
(3) Aronson, B. J.; Blanford, C. F.; Stein, A. *Chem. Mater.* **1997**, *9*, 2842.
(4) Prakash, A. M.; Sung-suh, H. M.; Kevan, L. *J. Phys. Chem. B* **1998**, *102*, 857.
(5) Maschmeyer, T.; Rey, F.; Sankar, G.; Thomas, J. M. *Nature* **1995**, *378*, 159.
(6) Huybrechts, D. R. C.; Bruycher, L. D.; Jacobs, P. A. *Nature* **1990**, *345*, 240.
(7) Morey, M. S.; O'Brien, S.; Schwarz, S.; Stucky, G. D. *Chem. Mater.* **2000**, *12*, 898.
(8) Luan, Z.; Maes, E. M.; Vander Heide, P. A. W.; Zhao, D. Y.; Czernuszewicz, R. S.; Kevan, L. *Chem. Mater.* **1999**, *11*, 3680.
(9) Jansen, J. C., Stocker, M., Karge, H. G., Weitkamp, J., Eds. *Studies in Surface Science and Catalysis*; Elsevier: Amsterdam, The Netherlands, 1994; Vol. 85, pp 177−213.
(10) Prakash, A. M.; Kurshev, V.; Kevan, L. *J. Phys. Chem.* B **1997**, *101*, 9794.
(11) Kresge, C. T.; Leonowicz, M. E.; Roth, W. J.; Vartuli, J. C.; Beck, J. S. *Nature* **1992**, *359*, 710.
(12) Shen, Y. F.; Zerger, R. P.; Deguzman, R. N.; Suib, S. L.; McCurd, L.; Potter, D. I.; O'Yong, C. L. *Science* **1993**, *260*, 511.
(13) Tanabe, K.; Yamaguchi, T. *Catal. Today* **1994**, *20*, 185.
(14) Tanabe, K.; Misono, M.; Ono, Y.; Hattori, H. *Stud. Surf. Sci. Catal.* **1989**, *51*, 1.
(15) Boyse, R. A.; Ko, E. I. *Catal. Lett.* **1996**, *38*, 225.
(16) Ciesla, U.; Schacht, S.; Stucky, G. D.; Unger, K. K.; Schuth, F. *Angew. Chem., Int. Ed. Engl.* **1996**, *35*, 541.
(17) Romannikov, V. N.; Fenelonov, V. B.; Paukshtis, E. A.; Derevyankin, A. Yu.; Zaikovskii, V. Z. *Microporous Mesoporous Mater.* **1998**, *21*, 411.

10.1021/cm000798l CCC: $20.00
Published on Web 02/23/2001

with the doping of porous zirconium oxide have attracted much interest.[19] For example, aluminum-doped mesoporous zirconia would help to increase the thermal stability and preserve its surface area.[20] This paper describes the incorporation with variable amounts of titanium into the framework of ordered porous zirconium oxide molecular sieves by direct-hydrothermal synthesis procedures. X-ray powder diffraction (XRD), nitrogen adsorption, diffuse reflectance ultraviolet, X-ray photoelectron (XPS), and Raman spectroscopies were used to characterize these incorporated samples.

2. Experimental Procedure

2.1. Materials Synthesis. The ordered porous Ti−zirconium oxides were prepared by direct synthesis, via the surfactant templating synthesis route. The titanium source was titanium isopropoxide (98%, Aldrich). $Zr(SO_4)_2 \cdot 4H_2O$ was used as the Zr source and hexadecyltrimethylammonium bromide (C_{16}TMABr) as the surfactant. The synthesis was carried out as follows: C_{16}TMABr (3.2 g, 8.7 mmol) was dissolved in a HCl solution (0.1 M), and $Zr(SO_4)_2 \cdot 4H_2O$ (16.85 g, 47.4 mmol) dissolved in H_2O (75 g) was added into the surfactant solution at a rate of 30 mL/h during stirring. At the same time, titanium isopropoxide (*x* mL) was added at the rate of 6 mL/h while stirring. The mixture was stirred for at least 3 h and aged for another 3 h at room temperature. Then the mixture was removed into a closed polypropylene bottle with hydrothermal treating at 110 °C for 48 h. The obtained precipitate was filtered and dried at 100 °C. The as-synthesized material was stirred for 3 h in a 0.5 M phosphoric acid solution (85 wt %). After filtering, washing, and drying, the surfactant was removed by calcination under flowing air at 773 K for 6 h. The material thus obtained was a white powder. In the above synthesis, the Ti/Zr molar ratios were controlled at 0, 5%, 10%, 15%, 20%, 25%, 30%, and 40%, and the resultant corresponding materials were designated as T0, T0.5, T1, T1.5, T2, T2.5, T3, and T4, respectively.

2.2. Analysis. XRD patterns were obtained using a Rigaku D/max-RB diffractometer. Analyses were performed with Cu Target (40 kV and 60 mA); a typical scan speed was 5°/min with a step of 0.002°, in the range from 1.8° to 10°.

N_2 adsorption−desoption isotherms were obtained at 77.35 K on a Micromeritics Tristar 3000 analyzer. The samples were outgassed at 250 °C in flowing N_2 for at least 20 h before measurement.

HRTEM and EDS were measured with a JEOL 200CX electron microscope operated at 200 kV.

Diffuse reflectance UV−vis spectra were taken on a Shimadzu UV-3101PC UV−vis−NIR scanning spectrophotometer, equipped with an integrating sphere using $BaSO_4$ as the reference.

Raman spectra were obtained at room temperature using a 1064 nm line from a YAG laser beam on a Bio-RAD FT-Raman spectrometer.

XPS were collected on a VG Micro MK II instrument using monochromatic Mg Kα X-rays at 1254 eV operated at 300 W. The O(1s) binding energies were referenced to the C(1s) line situated at 284.6 eV.

3. Results and Discussion

Bulk structural characterization by XRD of porous ZrO_2 support (Figure 1a) incorporated by various amounts of titanium (Figure 1b−d) confirms that the structure is maintained upon hydrothermal incorporation of Ti by direct synthesis. It can be seen from Figure 1 that small amounts of Ti doping will help to increase the ordering of the pore structure. However, the ordering will decrease with further incorporation. Upon calcination at 773 K, the XRD peaks of these Ti−ZrO_2 samples shift to lower *d* spacing (Table 1), because the materials undergo further condensation and contraction of pores upon the removal of the surfactant. The XRD patterns for samples T0, T2, and T4 after calcination within the range of 10−80° are shown in Figure 2. It can be seen that sample T2 shows an XRD pattern similar to that of sample T0, and no characteristic peaks belonging to titania have been observed, while for sample T4 there is a distinctive peak at 25° belonging to titania. This suggests that some lattices of zirconium may be substituted by the introduction of titanium in small amounts; i.e., titanium can be incorporated into the inorganic wall of ZrO_2, while nanocrystalline titania would be separated out from the supporting material,

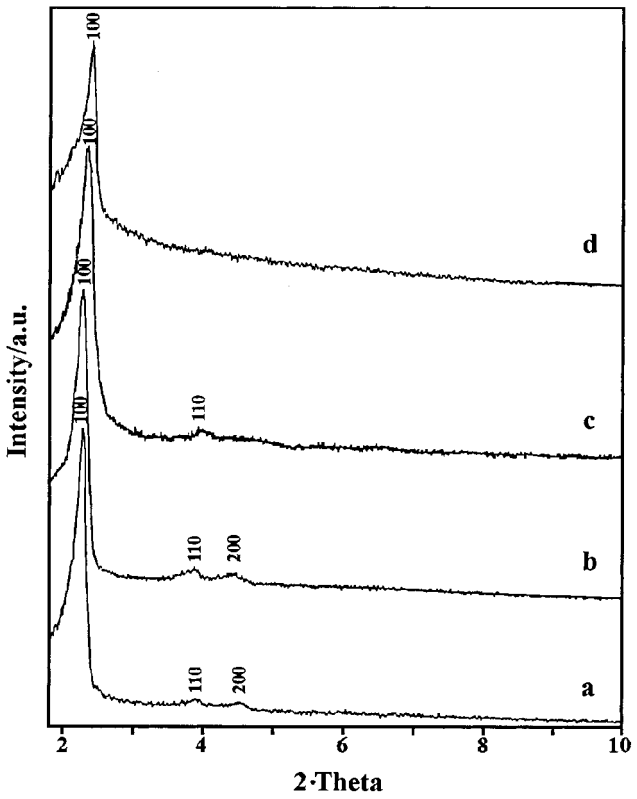

Figure 1. XRD patterns of samples (a) T0, (b) T2, (c) T3, and (d) T4.

Table 1. Pore Structure Parameters and the Results of X-ray Fluorescence Analysis for the Ti−ZrO_2 Samples with Varying Titanium Dopings

	sample					
	T0	T1	T2	T2.5	T3	T4
designated amount of Ti (mol %)	0	10	20	25	30	40
actual amount of Ti (mol %)	0	9.8	19.2	24.3	30	40
value of *d*(100) (nm)	3.14	3.18	3.15	3.14	3.07	2.95
a_0 value[a] (nm)	3.626	3.672	3.637	3.626	3.545	3.406
wall thickness[b] (nm)	1.756	1.802	1.787	1.766	1.695	1.556
pore volume (cm^3/g)	0.168	0.188	0.170	0.164	0.160	0.155
BET surface area (m^2/g)	360	402	368	352	345	334

[a] $a_0 = 2d(100)/\sqrt{3}$. [b] Wall thickness = a_0 − pore size. The pore size was determined by the adsorption average pore diameter.

(18) Wong, M. S.; Antonelli, D. M.; Ying, J. Y. *Nanostruct. Mater.* **1997**, *9*, 165.
(19) Mamak, M.; Coombs, N.; Ozin, G. *Adv. Mater.* **2000**, *12*, 198.
(20) Zhao, E.; Hardcastle, S. E.; Pacheco, G.; Garcia, A.; Blumenfeld, A. L.; Frepiat, J. J. *Microporous Mesoporous Mater.* **1999**, *31*, 9.

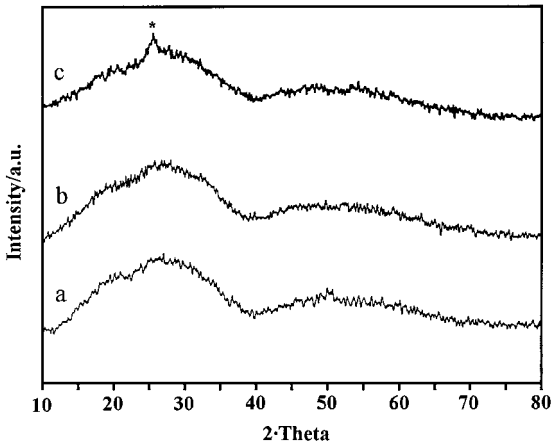

Figure 2. XRD patterns for the samples within the range of 10−80° after calcination at 773 K for 6 h: (a) T0, (b) T2, (c) T4.

once the doping level of titanium is higher than 20 mol %.

The actual amounts of Ti (mol %) of these samples analyzed by X-ray fluorescence are very close to their designated ratios (Table 1). This means that titanium can be effectively incorporated into the porous ZrO_2 via the direct-hydrothermal synthesis procedure. The nitrogen adsorption isothermals measured at 77.35 K of samples T0, T1, T2, and T4 are shown in Figure 3. All of these four samples synthesized with C_{16} surfactant show the type I isothermal, which is an indication for the presence of pores with sizes between micro- and mesopores.[16] The BET surface area of porous ZrO_2 is around 360 m^2/g after calcination at 773 K, and the value increases up to 402 m^2/g with 10 mol % of Ti incorporation, which is in good agreement with the values of d(100) spacing from the XRD results. Furthermore, both the pore volume and the wall thickness for samples T1 and T2 are higher than those of the T0 sample, which suggests that a suitable amount of Ti doping (less than 20 mol %) will help to increase the thermal stability of porous zirconium oxide. This can be associated with the improved condensation of the zirconium framework owing to the incorporation of TiO_3^{2-}. The comparison of the BET surface areas for samples T0 and T1 at different calcining temperatures has been shown in our previous work.[21] The variation of the a_0 values and the wall thickness indicates that the hexagonal unit cell dimension would be changed with the doped amount of titanium. The BET surface areas and the values of d spacing as well as the wall thickness decrease when the Ti doping is higher than 30 mol %, which may be due to the decrease of the ordering structure, because of the much higher amount of Ti doping.

Figure 4 shows the representative HRTEM image of sample T2 and the corresponding EDS measurement (Figure 4b). As can be seen in the TEM image, a well-ordered pore structure is still maintained after calcination at 773 K. Furthermore, neither visible nanoparticles of titania nor diffuse intensity and superlattice reflections could be observed in this image as well as in the selected area electron diffraction pattern. However, the distinctive signal of titanium is detected by the corresponding EDS measurement, which indicates that the introduction of titanium may have been incorporated into the framework of zirconium oxide. Figure 5 shows the TEM image of a local area of sample T4 (Figure 5a) and the corresponding EDS measurement (Figure 5b). It is clear that a large amount of nanocrystalline TiO_2 is present on the supporting material and the intensity of the Ti signal measured by EDS is much higher than that of sample T2. Further evidence for the incorporation of titanium into the framework of zirconia can be found from the following demonstration.

Raman spectroscopy is an effective tool for determining the presence or absence of extraframework TiO_2 nanoparticles, because it is extremely sensitive to crystalline forms of TiO_2 because of its strong scattering properties.[22] Raman spectra for the bands at 638, 514, 394, and 144 cm^{-1} belong to the characteristic absorbance of the anatase TiO_2.[7] Particularly, the remarkably strong band at 144 cm^{-1} can be used to evaluate the

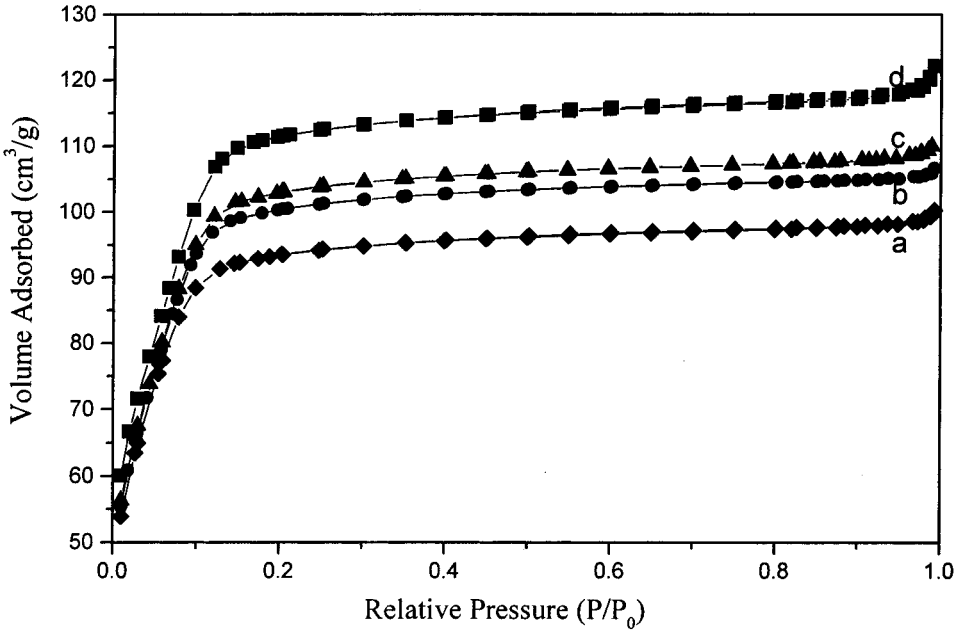

Figure 3. N_2 adsorption−desorption isothermals of samples (a) T4, (b) T0, (c) T2, and (d) T1.

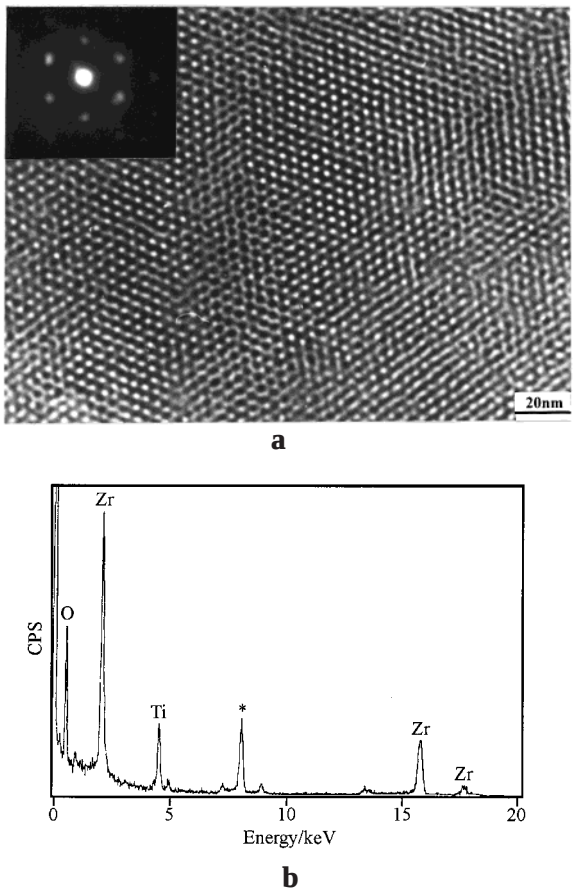

Figure 4. (a) TEM image of sample T2 and its selected area electron diffraction pattern. (b) Corresponding EDS spectrum (* is the Cu element), which arises from the supporting grid.

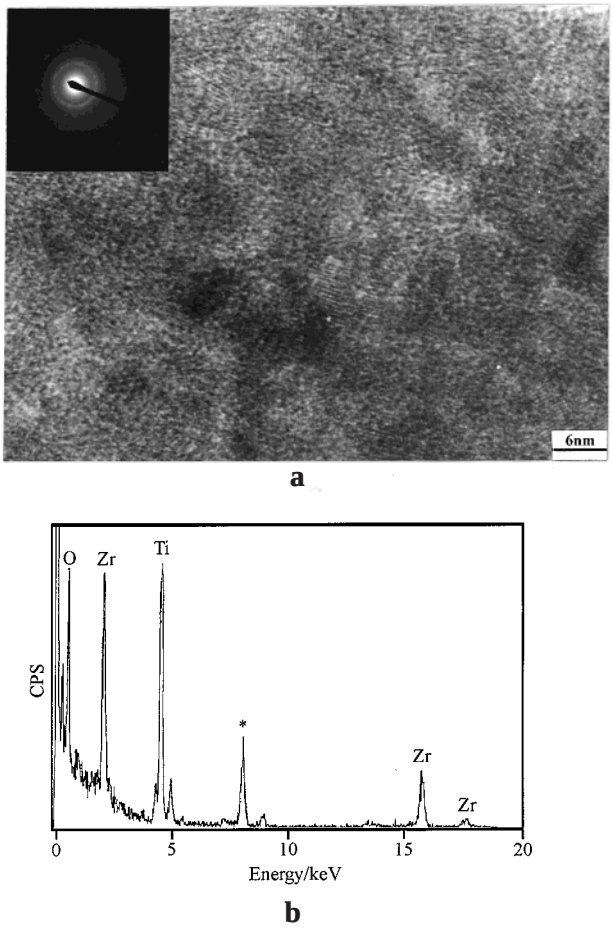

Figure 5. (a) TEM image of the local area of sample T4 and its electron diffraction pattern. (b) Corresponding EDS spectrum.

amount of extralattice Ti present in porous ZrO_2. In Figure 6b,c, no sign of the absorbance at 144 cm^{-1} can be observed, confirming the absence of extraframework bulk crystalline titania. However, the intense Raman signal occurs at 144 cm^{-1} for higher titanium loading (Figure 6d,e), which is characteristic of TiO_2 anatase particles. It is worth noting that the Raman absorbent peak at around 835 cm^{-1} occurs and the intensity increases with the Ti-doping level (Figure 6a−c), when the doping level is less than 20 mol %. As the incorporated amount of titanium further increases, a similar intensity is maintained (Figure 6d,e). Therefore, the band at around 835 cm^{-1} is believed to be related solely to the Ti−O−Zr bonding in the inorganic framework of ZrO_2. The Raman spectra also suggest that isolated titanium ions are present in the framework of supporting material with the titanium loading at not higher than 20 mol %. Meanwhile, the extraframework of anatase TiO_2 appears when the Ti loading gets higher.

Figure 7 shows O(1s) XPS spectra of Ti−ZrO_2 samples with varying titanium loadings. The T0 sample shows an O(1s) line at 531.5 eV binding energy, which is about 1.3 eV higher than that of TiO_2 anatase.[8] With increased titanium loading, the position of the O(1s) lines shift toward lower binding energies, which can be attributed to oxygen presence in different environments from its presence in pure porous zirconium oxide. It is noted that the binding energy of the O(1s) line of the T0 sample gets a relatively distinctive decrease at increased Ti doping up to 20 mol %. This can be explained by the fact that some zirconium was replaced by titanium, which induced the decrease of interatomic potentials due to the reduction of the overall atomic size.

Figure 8 shows Zr(3d) XPS spectra as a Zr($3d_{5/2}$) and Zr($3d_{3/2}$) doublet with a separation of 2.4 eV[23] for porous ZrO_2 with varying titanium loadings. At low titanium loading, T2 shows a Zr($3d_{5/2}$) line at 182.72 eV binding energy, which is about 0.5 eV lower than that of undoped sample T0. As the titanium loading further increases for sample T3, the position of the Zr($3d_{5/2}$) line at 182.75 eV is very close to that for sample T2. This suggests a homogeneous dispersion of Ti(IV) ions in the framework of ZrO_2, at a titanium loading not higher than 20 mol %. With the further increases of the titanium loading above 20 mol %, the chemical environment of zirconium remains almost unchanged. This further confirms that the additional titanium loading higher than 20 mol % cannot be further incorporated into the framework of the ZrO_2 wall. The XPS result of the upper limit of 20 mol % Ti doping in the framework of the ZrO_2 wall is consistent with the Raman spectra, which is much higher than the possible Ti loading in silica-based materials.[7,8]

(21) Chen, H. R.; Shi, J. L.; Yu, J.; Wang, L. Z.; Yan, D. S. *Microporous Mesoporous Mater.* **2000**, *39*, 171.

(22) Gao, X.; Bare, S. R.; Fierro, J. L. G.; Banares, M. A.; Wachs, I. E. *J. Phys. Chem. B* **1998**, *102*, 5653.

(23) *Handbook of X-ray photoelectron spectroscopy*; Chastain, J., King, R. C., Jr., Eds.; Physical Electronics, Inc.: Minneapolis, MN, 1995.

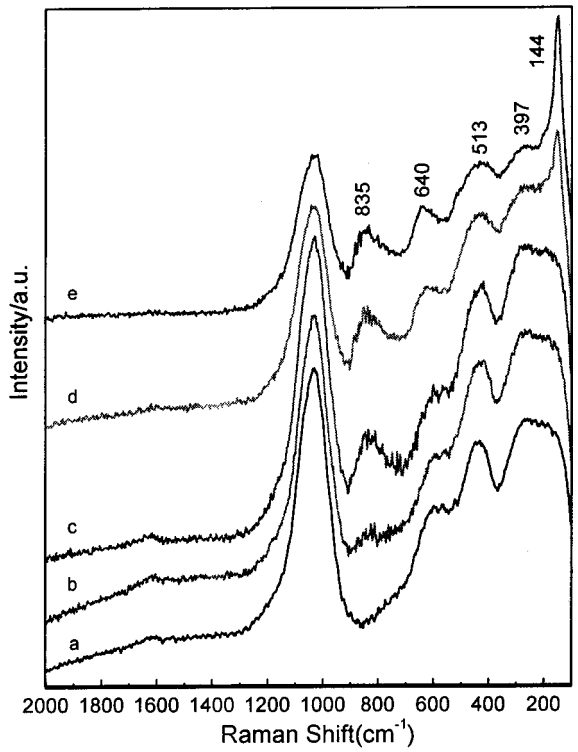

Figure 6. Raman spectra of Ti−ZrO_2 materials with varying titanium doping corresponding to samples (a) T0, (b) T0.5, (c) T2, (d) T3, and (e) T4.

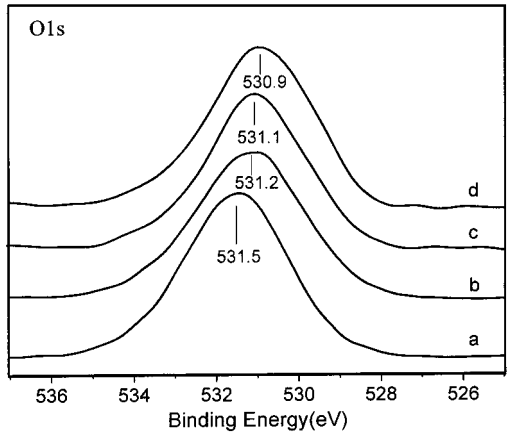

Figure 7. O(1s) XPS spectra of Ti−ZrO_2 materials with varying titanium doping corresponding to samples (a) T0, (b) T2, (c) T3, and (d) T4.

UV−vis absorption spectroscopy has been extensively used to characterize the nature and coordination of titanium ions in titanium-substituted molecular sieves.[24,25] Figure 9 shows UV−vis spectra of the series of Ti-incorporated samples. As illustrated, the undoped sample T0 shows a very weak absorption peak at 210 nm. For the referent sample of pure TiO_2 anatase, a broad absorption at 330 nm is found. The ultraviolet absorption wavelength of titanium is sensitive to its coordination and to the TiO_2 particle size.[26] At low Ti loading corresponding to sample T0.5, the observed absorption peak is at 230 nm, presenting neither the absorption of ZrO_2 nor the absorption of TiO_2, and with

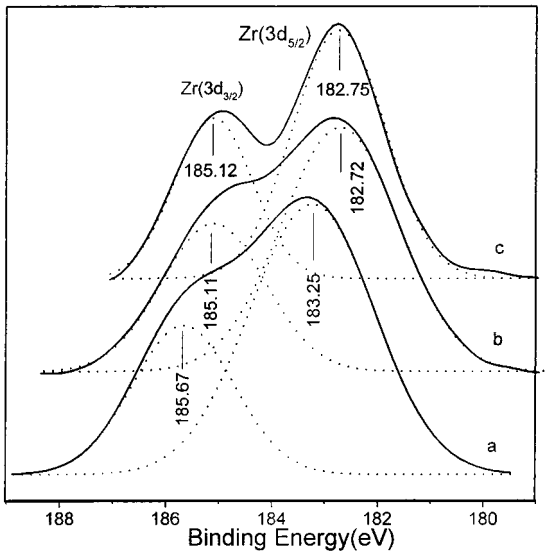

Figure 8. Zr(3d) XPS spectra of Ti−ZrO_2 materials with varying titanium doping corresponding to samples (a) T0, (b) T2, and (c) T3.

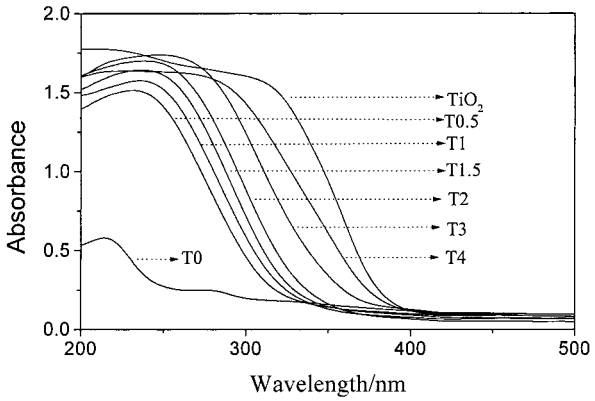

Figure 9. UV−vis spectra of Ti−ZrO_2 samples with varying titanium doping and the referent sample of bulk TiO_2 anatase.

the intensity remarkably increased. This suggests that Ti(IV) has effectively modified the Zr−O−Zr coordination; i.e., Ti(IV) has been incorporated into the framework of ZrO_2.[21] Furthermore, the increased intensity of absorption peaks and the red-shifted magnitude of the adsorption bands correspond well to the amount of the Ti incorporation when the amount of Ti doping is less than 20 mol %. This may prove that titanium can be homogeneously dispersed into the framework of ZrO_2. Also, the gradual red shift can be related to a transition for the coordination of titanium ions from Zr−O−Ti coordination to the octahedral coordination of TiO_2. The abnormal absorption curve of sample T4 in this figure may be caused by the surplus TiO_2 dispersed onto the outer surface of ZrO_2. Relative to bulk TiO_2 anatase, the broad absorption band of sample T4 blue shifted from 330 to 300 nm. A similar case was found in dispersed TiO_2 nanoparticles on the mesoporous silica materials.[8,22]

4. Conclusion

A direct and effective synthetic method for the incorporation of titanium into the framework of ordered porous zirconium oxide has been demonstrated. Both bulk structural characterizations and spectroscopy re-

(24) Luan, Z.; Kevan, L. *J. Phys. Chem. B* **1997**, *101*, 2020.
(25) Corma, A.; Navarro, M. T.; Pariente, J. P. *J. Chem. Soc., Chem. Commun.* **1994**, 147.
(26) Davis, R. J.; Liu, Z. *Chem. Mater.* **1997**, *9*, 2311.

sults reveal that titanium is homogeneously dispersed into the framework of a porous ZrO_2 wall at a low titanium loading level and the upper limit of Ti incorporation into the framework of ZrO_2 is 20 mol % higher than that in silica-based materials. The experimental results show that the pore structure and the high surface area are still maintained with Ti incorporation. The proper amount of Ti doping is helpful for the improvement of the thermal stability of porous ZrO_2 material, whereas nanocrystalline TiO_2 anatase is formed at titanium loading above 20 mol %. These new Ti−ZrO_2 materials may be potentially useful as a novel catalyst.

Acknowledgment. This work was supported by the National Natural Science Foundation of China with Contract 59882007.

CM000798L